Chemical Physics 370 (2010) 258–269

Contents lists available at ScienceDirect

Chemical Physics

journal homepage: www.elsevier.com/locate/chemphys

# Noise-induced dynamic symmetry breaking and stochastic transitions in ABA molecules: II. Symmetric–antisymmetric normal mode switching

Maksym Kryvohuz, Jianshu Cao *

*Department of Chemistry, Massachusetts Institute of Technology, Cambridge, MA 02139, USA*

ARTICLE INFO

*Article history:*
Received 6 October 2009
In final form 24 February 2010
Available online 1 March 2010

*Keywords:*
Dynamic symmetry breaking
Stochastic transitions
Symmetric-to-antisymmetric normal mode switching
Environment induced dephasing
Triatomic ABA molecules

ABSTRACT

The second paper of the series discusses the effect of thermal noise on the stretching vibrational dynamics of symmetric triatomic ABA molecules. In particular, noise-induced transitions between symmetric and antisymmetric normal-mode vibrations are discussed, in the context of symmetry breaking of vibrational dynamics. The statistics of symmetry breaking transitions and the average lifetimes of normal modes of different symmetries are derived analytically and compared with direct numerical simulations. The average lifetimes of symmetric and antisymmetric normal modes are found to be inversely proportional to bath friction strength and depend on the dimensionless parameter $\kappa$ which is the combination of bath temperature, bond anharmonicity and bond–bond coupling strength. Antisymmetric normal mode depends weakly on $\kappa$ and is always stable. Symmetric normal mode depends significantly on $\kappa$ and becomes unstable at $\kappa = 1$. Higher temperatures destabilize symmetric normal mode and therefore decrease the ratio of symmetric-to-antisymmetric normal mode populations contrary to intuitive expectation.



## 1. Introduction

In the previous paper [1], hereafter referred to as paper **I**, we considered a model of ABA molecule in the form of two linearly coupled Morse oscillators. We refer reader to the paper **I** for discussion of the model and review of the literature. We have numerically observed, that ABA model coupled to the bath of harmonic oscillators switches intermittently between the four distinct vibrational modes along its dynamic trajectory, resulting in blinking of vibrational bond energy. The statistics of these dynamic transitions (i.e., 'vibrational blinking') such as noise-induced symmetry breaking [2,3] and activated barrier crossing [4] is the subject of theoretical analysis in the present and the following papers, respectively. The observed rich dynamic behavior can be relevant for understanding the stochasticity of energy localization in complex systems ranging from polyatomic molecules to nano-structures and micro-mechanical oscillators [5].

The classical stretching vibrational dynamics of ABA molecules at all energies can be effectively described by the hamiltonian of a hindered rotor [6–8] with momentum-dependent potential [1,9,10]

$$H_{rot} = \frac{p^2}{2M} + W_0\sqrt{J_+^2 - p^2}\cos(2\psi). \tag{I.1}$$

For a non-dissipative ABA system, the parameter $J_+$, which stands for the total number of vibrational quants in AB and BA Morse oscillators, is a constant. This parameter determines the probability of a particular type of vibrational dynamics in ABA molecules, i.e. local- or normal-mode dynamics. If $J_+ < MW_0$, only normal-mode dynamics is possible for ABA molecules and both symmetric and antisymmetric normal modes are stable. If $MW_0 < J_+ < 2MW_0$ antisymmetric and symmetric normal modes are stable and a special type of stable local mode termed "quasi-local" mode appears. If $J_+ > 2MW_0$ all vibrational modes (local, quasi-local and antisymmetric normal) are present except for symmetric vibrational mode, which is unstable in this energy range. The stability analysis of different types of modes in isolated ABA molecules were also studied extensively in [9–11]. The dynamical picture of ABA vibrations becomes much more interesting if we consider ABA molecules subjected to external noise from thermal environment, which defines the purpose of this study.

The local mode dynamics of ABA molecules corresponds (disregarding the special case of "quasi-local" modes) to free rotation of rotor (I.1) above its cosine potential, $E_{rot} > W_0 J_+$ [1,6,7]. Normal mode dynamics of ABA molecules corresponds to hindered motion of rotor, i.e. oscillations in cosine potential, $E_{rot} < W_0 J_+$. Since the normal-mode dynamics of ABA molecule corresponds to the confined motion in dynamical cosine potential, noise from environment should result in the escape from the confining cosine potential according to the Kramers mechanism of noise-driven escape [12]. When escaping from the cosine potential, the dynamics of ABA molecules therefore switches from normal-mode vibrations

* Corresponding author.
*E-mail addresses:* maximian@caltech.edu (M. Kryvohuz), jianshu@mit.edu (J. Cao).

0301-0104/$ - see front matter © 2010 Elsevier B.V. All rights reserved.
doi:10.1016/j.chemphys.2010.02.024

to local-mode vibrations. This simple picture illustrates how external noise can influence vibrational dynamics of ABA molecules. In fact, the noise from environment induces the ABA system to switch between all possible types of vibrational motion, i.e. antisymmetric normal modes, symmetric normal modes, local and quasi-local modes, as we showed numerically in paper **I**. These noise-induced transitions are stochastic dynamical transitions (SDT) of vibrational modes and will be analyzed in papers II and III.

In the present paper, we discuss a particular type of SDT, which is symmetric-to-antisymmetric normal mode transitions and will, in paper III, discuss the other types of SDT and the overall analytical picture of SDT. As we show below, these SDTs are the dominant dynamical transitions in the temperature range of interest. In paper **I**, we have numerically observed a non-statistical distribution of the lifetimes of symmetric and antisymmetric normal modes as well as weak dependence of the lifetime of antisymmetric normal mode on the bath temperature and AB–BA bond coupling strength. In paper II, we present an analytical theory to explain the observed effects. The paper is organized as follows: in Section 2, we derive the effective Langevin equations that describe the noise-induced dynamical symmetry breaking. In Sections 3 and 4, we reduce the obtained Langevin equations to the one-dimensional energy-diffusion equation. In Sections 5 and 6, we solve the derived diffusion equation to obtain the statistics of symmetry breaking dynamical transitions and compare it with the direct numerical simulations. We discuss the obtained results in Section 7.

## 2. The effective Langevin equation

In paper **I**, we described a dissipative ABA molecule as a system of two coupled anharmonic oscillators individually coupled to a bath of harmonic oscillators (Gaussian bath)

$$H = H_{ABA} + H_{b1} + H_{b2}, \tag{II.1}$$

where

$$H_{ABA} = \frac{1}{2}G_{11}p_1^2 + U(x_1) + \frac{1}{2}G_{11}p_2^2 + U(x_2) + G_{12}p_1p_2 \tag{II.2}$$

is the Hamiltonian of the two kinetically coupled Morse oscillators with $U(x) = D(1-e^{-\alpha x})^2$, $G_{11} = (m_A+m_B)/m_Am_B$, $G_{12} = \frac{\cos(\theta_{ABA})}{m_B}$ and

$$H_{bi} = \sum_j \left(\frac{P_j^2}{2} + \frac{1}{2}\omega_j^2\left(Q_j - \frac{\gamma_j}{\omega_j^2}x_i\right)^2\right) \tag{II.3}$$

is the Hamiltonian of a Gaussian bath. For the Ohmic distribution of bath frequencies, the dynamics of an ABA molecule is governed by a set of stochastic equations

$$\begin{aligned}
\frac{dx_1}{dt} &= G_{11}p_1 + G_{12}p_2,\\
\frac{dp_1}{dt} &= -\frac{dU(x_1)}{dx_1} - \gamma p_1 - \gamma\frac{G_{12}}{G_{11}}p_2 + F_1(t),\\
\frac{dx_2}{dt} &= G_{11}p_2 + G_{12}p_1,\\
\frac{dp_2}{dt} &= -\frac{dU(x_2)}{dx_2} - \gamma p_2 - \gamma\frac{G_{12}}{G_{11}}p_1 + F_2(t),
\end{aligned} \tag{II.4}$$

where

$$\langle F(t)F(t')\rangle = \frac{2\gamma kT}{G_{11}}\delta(t-t'). \tag{II.5}$$

Here $\gamma$ is the friction coefficient and $T$ is the temperature. We now write down the Kramers/Smoluchowski equation for the probability density $\rho(t;x_1,x_2,p_1,p_2)$ that corresponds to the Langevin equation (II.4):

$$\begin{aligned}
\frac{\partial\rho}{\partial t} = \Big[&-(G_{11}p_1+G_{12}p_2)\frac{\partial}{\partial x_1} + U'(x_1)\frac{\partial}{\partial p_1} - (G_{11}p_2+G_{12}p_1)\frac{\partial}{\partial x_2}\\
&+ U'(x_2)\frac{\partial}{\partial p_2} + \gamma\frac{G_{12}}{G_{11}}p_1\frac{\partial}{\partial p_2} + \gamma\frac{G_{12}}{G_{11}}p_2\frac{\partial}{\partial p_1}\\
&+ \gamma\frac{\partial}{\partial p_1}\left(p_1 + \frac{kT}{G_{11}}\frac{\partial}{\partial p_1}\right) + \gamma\frac{\partial}{\partial p_2}\left(p_2 + \frac{kT}{G_{11}}\frac{\partial}{\partial p_2}\right)\Big]\rho.
\end{aligned} \tag{II.6}$$

The first four terms in Eq. (II.6) is the Louville operator $\widehat{L} = -i\{\ldots, H_{ABA}\}$ which in the absence of noise $\gamma = 0$ propagates deterministic (reversible) classical trajectories $\partial\rho/\partial t + i\widehat{L}\rho = 0$. The last two terms are one-dimensional irreversible operators $\widehat{L}_{irr} = \gamma\frac{\partial}{\partial p}(p + \frac{kT}{G_{11}}\frac{\partial}{\partial p})$. Eq. (II.6) can thus be rewritten in a simpler form:

$$\frac{\partial\rho}{\partial t} = -\widehat{L}\rho + (\widehat{L}_{irr1} + \widehat{L}_{irr2})\rho + \gamma\frac{G_{12}}{G_{11}}\left(p_1\frac{\partial}{\partial p_2} + p_2\frac{\partial}{\partial p_1}\right)\rho, \tag{II.7}$$

where the last term appears due to the specific form of coupling in our problem – momentum coupling. In fact, as shown below, this term can be neglected if $G_{12}/G_{11} \ll 1$.

For the problem of SDT, we assume that the dissipative ABA molecule retains well-defined oscillating dynamics, which means that both the friction $\gamma$ and the temperature $T$ should be *small* in order not to disturb system's oscillatory nature, i.e. $kT \ll D$, $\gamma \ll \Omega$. Since we are considering the low-friction case, the appropriate variables for the diffusion problem (II.7) are the action-angle variables [12]. The following canonical transformations

$$\begin{aligned}
J_+ &= J_1 + J_2,\\
J_- &= J_1 - J_2,\\
\psi_+ &= (\varphi_1 + \varphi_2)/2,\\
\psi_- &= (\varphi_1 - \varphi_2)/2,
\end{aligned} \tag{II.8}$$

convert the ABA Hamiltonian to [1]

$$H_{ABA} = \Omega J_+ - \frac{\Omega^2 J_+^2}{8D} - \frac{\Omega^2 J_-^2}{8D} + \frac{G_{12}}{G_{11}}\frac{\Omega}{2}\sqrt{J_+^2 - J_-^2}\cos(2\psi_-), \tag{II.9}$$

where $J_i = J_i(x_i,p_i)$ and $\varphi_i = \varphi_i(x_i,p_i)$ are the action-angle variables of the Morse oscillator [13]. We now use these transformations to replace phase space variables $\{x_1,p_1,x_2,p_2\}$ in (II.7) with action-angle variables $\{\psi_-,J_-,\psi_+,J_+\}$. In doing so, we note that our system's Hamiltonian (II.9) does not depend on $\psi_+$, so we can average Eq. (II.7) over $\psi_+$. The possibility of averaging the Fokker–Planck equation over $\psi_+$ is the central result of this section. We perform this averaging over each of three terms in (II.7) as shown in Appendix A and obtain:

$$\begin{aligned}
\frac{\partial\bar{\rho}}{\partial t} = &-\{H_{ABA},\bar{\rho}\}_- + \gamma\frac{\partial}{\partial J_+}\left(J_+ - \frac{2kT}{\Omega}\right)\bar{\rho} + \gamma\frac{\partial}{\partial J_-}(J_-\bar{\rho})\\
&+ \frac{\gamma kT}{\Omega}\left(\frac{\partial^2}{\partial J_+^2}(J_+\bar{\rho}) + 2\frac{\partial^2}{\partial J_+\partial J_-}(J_-\bar{\rho}) + \frac{\partial^2}{\partial J_-^2}(J_+\bar{\rho})\right),
\end{aligned} \tag{II.10}$$

From here we now restore stochastic equations for $\{\psi_-,J_-,J_+\}$. In this case the diffusion matrix is

$$D = \frac{\gamma kT}{\Omega}\begin{pmatrix} 0 & 0 & 0\\ 0 & J_+ & J_-\\ 0 & J_- & J_+\end{pmatrix}.$$

Since $J_-$ can take negative values, the square root of matrix elements is not well-defined. We use the method of orthogonal transformation of diffusion matrix described in [14] (see Eq. (3.124)). Diagonalizing diffusion matrix $D$, taking positive root and transforming it back, we get:

$$D^{1/2} = \frac{1}{2}\sqrt{\frac{\gamma kT}{\Omega}}\begin{pmatrix} 0 & 0 & 0 \\ 0 & (\sqrt{J_+ + J_-} + \sqrt{J_+ - J_-}) & (\sqrt{J_+ + J_-} - \sqrt{J_+ - J_-}) \\ 0 & (\sqrt{J_+ + J_-} - \sqrt{J_+ - J_-}) & (\sqrt{J_+ + J_-} + \sqrt{J_+ - J_-}) \end{pmatrix} \equiv \begin{pmatrix} 0 & 0 & 0 \\ 0 & g_{11} & g_{12} \\ 0 & g_{12} & g_{11} \end{pmatrix}.$$

Therefore, the resulting stochastic equations (in Ito representation) are

$$\frac{d\psi_-}{dt} = \frac{\partial H_{ABA}}{\partial J_-}, \tag{II.11}$$

$$\frac{dJ_-}{dt} = -\frac{\partial H_{ABA}}{\partial \psi_-} - \gamma J_- + g_{11}\Gamma_1(t) + g_{12}\Gamma_2(t), \tag{II.12}$$

$$\frac{dJ_+}{dt} = -\gamma J_+ + \gamma\frac{2kT}{\Omega} + g_{12}\Gamma_1(t) + g_{11}\Gamma_2(t), \tag{II.13}$$

where random forces $\Gamma_i(t)$ obey $\langle\Gamma_i(t)\Gamma_j(t')\rangle = 2\delta_{ij}\delta(t-t')$ and $g_{11}$, $g_{12}$ are functions of both $J_-$ and $J_+$. Since Eqs. (II.11) and (II.12) contain partial derivatives of $H_{ABA}$ only over $J_-$ and $\psi_-$ we can replace $H_{ABA}$ in (II.9) with $-H_{rot}$ to have:

$$\frac{d\psi_-}{dt} = -\frac{\partial H_{rot}}{\partial J_-}, \tag{II.14}$$

$$\frac{dJ_-}{dt} = \frac{\partial H_{rot}}{\partial \psi_-} - \gamma J_- + g_{11}\Gamma_1(t) + g_{12}\Gamma_2(t), \tag{II.15}$$

$$\frac{dJ_+}{dt} = -\gamma J_+ + \gamma\frac{2kT}{\Omega} + g_{12}\Gamma_1(t) + g_{11}\Gamma_2(t), \tag{II.16}$$

where

$$H_{rot} \equiv \frac{\Omega^2 J_-^2}{8D} - \frac{G_{12}}{G_{11}}\frac{\Omega}{2}\sqrt{J_+^2 - J_-^2}\cos(2\psi_-), \tag{II.17}$$

is the last two terms in Eq. (II.9) and corresponds to the hindered rotor Hamiltonian (I.1).

Eqs. (II.14)–(II.16) describe all dynamic behavior of the dissipative ABA molecule in the interesting limit of weak friction limit. To proceed further with the analysis we need to specify the characteristic scales of the physical quantities and parameters that appear in Eqs. (II.14)–(II.16).

## 3. The magnitudes of parameters

The Langevin equations (II.14)–(II.16) correspond to the dissipative motion of a hindered rotor in the momentum-dependent cosine potential discussed in paper **I**. To estimate the magnitudes of the parameters of this dissipative motion we restrict ourselves to the case when the rotor oscillates in the cosine potential near its minimum at $\psi_- = \pi/2$ (antisymmetric normal mode). In this case we can set $J_- \ll J_+$, which simplifies Eqs. (II.14) and (II.15) to:

$$\frac{d\psi_-}{dt} = -\frac{\Omega^2 J_-}{4D}, \tag{III.1}$$

$$\frac{dJ_-}{dt} = -\gamma J_- + \frac{\Omega G_{12}}{G_{11}}J_+\sin(2\psi_-) + \sqrt{\frac{\gamma kTJ_+}{\Omega}}\Gamma_1(t). \tag{III.2}$$

Combining these equations we obtain the reduced Langevin equation:

$$\frac{4D}{\Omega^2}\ddot{\psi}_- = -\gamma\frac{4D}{\Omega^2}\dot{\psi}_- - \frac{G_{12}}{G_{11}}\Omega J_+\sin(2\psi_-) + \sqrt{\frac{\gamma kTJ_+}{\Omega}}\Gamma_1(t). \tag{III.3}$$

Although $J_+$ is a stochastic variable for the purpose of estimation, we can take it to be its average value, which from Eq. (II.16) is $\langle J_+\rangle = \frac{2kT}{\Omega}$. Eq. (III.3) describes dissipative oscillations of a particle of mass $M = \frac{4D}{\Omega^2}$ in the cosine potential well of the depth $E_b = \Omega J_+\frac{G_{12}}{G_{11}} \approx 2kT\frac{|G_{12}|}{G_{11}}$ with friction coefficient $\gamma$ and effective temperature $k\widetilde{T} = \frac{kTJ_+\Omega}{4D} \approx \frac{(kT)^2}{2D}$. If the temperature $k\widetilde{T}$ is comparable or higher than the barrier height $E_b$ (i.e. $\frac{kT}{4D}\frac{G_{11}}{|G_{12}|} > 1$) then the particle can almost freely escape from the cosine potential so that *no* confined motion inside the cosine potential is possible or no normal-mode dynamics of an ABA molecule can exist at this temperature. At these temperatures, thermal energy is greater than the coupling strength between AB and BA bonds, and thus these bonds will oscillate *independently*. For the normal-mode behavior of an ABA molecule, the rotor needs to spend considerable time in the cosine potential well, that implies, the condition $k\widetilde{T} \ll E_b$, or in other words:

$$\frac{kT}{D} \ll 4\frac{|G_{12}|}{G_{11}}. \tag{III.4}$$

The physical values of the critical temperature $4D\frac{|G_{12}|}{G_{11}}$ in (III.4) that corresponds to the strength of AB–BA bond coupling for different ABA molecules are shown in Table 1, indicating that condition (III.4) is valid for room temperatures. Yet, since, quantum mechanically, the energy of an ABA molecule cannot be lower than the zero-point energy the better agreement of the present classical analysis with quantum systems is expected for temperatures comparable to zero-point energies (the right column of Table 1).

As we have discussed in Section 1, the value of parameter $J_+$, which is now a stochastic variable for a dissipative ABA molecule, determines whether the normal-to-local mode transition is possible. The values of $J_+$, at which local modes can appear, were found to be $J_+ > MW_0 = \frac{2D}{\Omega}\frac{|G_{12}|}{G_{11}} \equiv \widetilde{J_+^c}$. Given (III.4) we can now compare the typical value of $J_+$ with its critical value:

$$\frac{\langle J_+\rangle}{\widetilde{J_+^c}} = \frac{\frac{2kT}{\Omega}}{\frac{2D}{\Omega}\frac{|G_{12}|}{G_{11}}} = \frac{kT}{D}\frac{G_{11}}{|G_{12}|} \ll 1. \tag{III.5}$$

Therefore (see Section 1) most of time the rotor will be trapped in the cosine potential without the possibility to escape. Thus the majority of SDT will be the transitions between the symmetric and antisymmetric normal modes, which we can also call dynamical symmetry breaking, see Fig. 1.

The normal mode motion of an ABA molecule corresponds to a oscillatory motion of the rotor in the cosine potential. To observe the periodic oscillations in the cosine potential (III.3) (and therefore to observe a normal-mode dynamics of an ABA molecule) we should have friction coefficient $\gamma$, smaller than the characteristic frequency $\widetilde{\Omega}$ of oscillation in the well. From (III.3), we find $\widetilde{\Omega} = \sqrt{\frac{|G_{12}|}{G_{11}}\frac{\Omega^3 J_+}{4D}} \approx \Omega\sqrt{\frac{|G_{12}|}{G_{11}}\frac{kT}{2D}}$ and thus

$$\gamma \ll \Omega\sqrt{\frac{|G_{12}|}{G_{11}}\frac{kT}{2D}}. \tag{III.6}$$

Now we can compare the time scales of evolution of variables $J_+$ and $J_-$ (see for instance Fig. 1). The characteristic time scale of the evolution of stochastic variable $J_+$ can be found from Eq. (II.16):

**Table 1**
Critical decoupling temperatures $4D\frac{|G_{12}|}{G_{11}}$ for different ABA molecules.

| Molecule | $\theta_e$ (deg) | $\frac{\lvert G_{12}\rvert}{G_{11}}$ | $D$ (K) | $4D\frac{\lvert G_{12}\rvert}{G_{11}}$ (K) | $E_{zp}$ (K) |
|---|---|---|---|---|---|
| $SO_2$ | 119 | 0.014 | 66,300 | 3750 | 800 |
| $D_2O$ | 104.5 | 0.028 | 60,300 | 6720 | 1950 |
| $H_2O$ | 104.5 | 0.015 | 64,000 | 3770 | 2660 |
| $CH_2$ | 102 | 0.016 | 50,000 | 3200 | 2090 |
| $H_2S$ | 92 | 0.001 | 45,200 | 200 | 1850 |

(a) $\theta_e$ is the equilibrium value of bending angle; (b) $\frac{|G_{12}|}{G_{11}}$ is the bond–bond coupling strength; (c) $D$ is the bond dissociation energy expressed in Kelvins; (d) the critical temperature from Eq. (III.4) above which the oscillations of AB and BA bonds can be considered decoupled; (e) $E_{zp} = \frac{1}{2}\hbar\omega_0$ – approximate value of zero-point energy of quantum oscillations in AB-bond potential expressed in Kelvins.

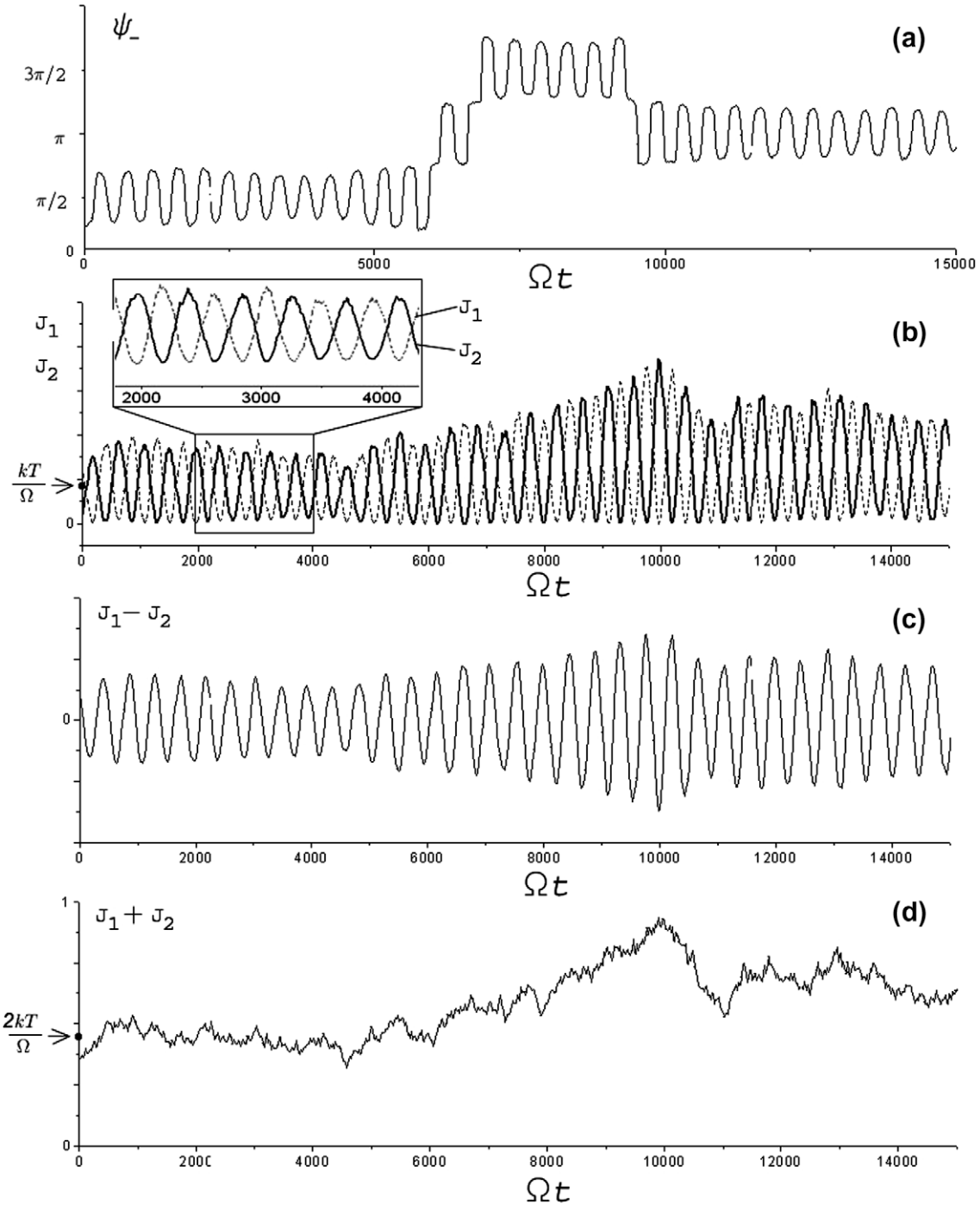


**Fig. 1.** A typical trajectory in action-angle variables that shows antisymmetric-to-symmetric normal mode transitions in ABA molecules as a function of dimensionless time $\Omega t$ (if divided by $2\pi$ it gives the number of normal-mode vibrations of the model $H_2O$ molecule). The plot (a) represents the time-dependence of AB and BA bond phase difference $\psi_- = (\phi_1 - \phi_2)/2$: the stable oscillations around $\psi_- = \pi/2, 3\pi/2$ indicate antisymmetric normal mode behavior, while the stable oscillations around $\pi$ correspond to symmetric normal-mode behavior. Plot (b) shows the corresponding time-dependence of the local action variables $J_1$ and $J_2$: the complete energy exchange between $J_1$ and $J_2$ indicates the normal-mode behavior. Plot (c) represents the difference of local actions $J_- = J_1 - J_2$, while plot (d) represents the sum of local actions $J_+ = J_1 + J_2$. Note the different timescales between $J_-$ of (c) and $J_+$ of (d).

$$\tau_+ = \frac{1}{\gamma}. \tag{III.7}$$

The characteristic time scale of evolution of $J_-$ is $1/\widetilde{\Omega}$, i.e.

$$\tau_- = \frac{1}{\Omega}\sqrt{\frac{G_{11}}{|G_{12}|}\frac{2D}{kT}}. \tag{III.8}$$

From the inequality (III.6) we can see that

$$\frac{\tau_-}{\tau_+} \ll 1, \tag{III.9}$$

indicating that $J_+$ changes *much slower* than $J_-$, thus we can consider $J_+$ as a slow variable that changes adiabatically with respect to fast variable $J_-$.

## 4. Reduction of stochastic equations

### 4.1. Decoupling of Langevin equation for $J_+$

Because of the difference in time scales, Eq. (III.9), the evolution of $J_+$ governed by Eq. (II.16) is decoupled from the evolution of $J_-$ governed by Eqs. (II.14) and (II.15). Indeed, since $J_-$ changes very rapidly, we can set its value in the equation for $J_+$ (II.16) to be equal to its average value $\langle J_-\rangle$, which is zero since $J_-$ changes its sign. Therefore, for $g_{ij}$ in Eq. (II.16) we can set $\sqrt{J_+ \pm J_-} \approx \sqrt{J_+ \pm \langle J_-\rangle} \approx \sqrt{J_+}$ resulting in $g_{12} = 0$, and $g_{11} = \sqrt{J_+}$. This finding decouples the system of Eqs. (II.14)–(II.16) into a self-consistent equation for $J_+$:

$$\frac{dJ_+}{dt} = -\gamma J_+ + \gamma\frac{2kT}{\Omega} + \sqrt{\frac{\gamma kTJ_+}{\Omega}}\Gamma_2(t), \tag{IV.1}$$

and equations for $J_-$ in which $J_+$ plays the role of a modulation parameter:

$$\frac{d\psi_-}{dt} = -\frac{\partial H_{rot}}{\partial J_-}, \tag{IV.2}$$

$$\frac{dJ_-}{dt} = \frac{\partial H_{rot}}{\partial \psi_-} - \gamma J_- + g_{11}\Gamma_1(t) + g_{12}\Gamma_2(t). \tag{IV.3}$$

The independent noise-term $g_{11}\Gamma_1(t) + g_{12}\Gamma_2(t)$ in (IV.3) can be approximated with a random force $\sqrt{g_{11}^2 + g_{12}^2}\Gamma(t) = \sqrt{\frac{\gamma kTJ_+}{\Omega}}\Gamma(t)$, resulting in equations:

$$\frac{d\psi_-}{dt} = -\frac{\partial H_{rot}}{\partial J_-}, \tag{IV.4}$$

$$\frac{dJ_-}{dt} = \frac{\partial H_{rot}}{\partial \psi_-} - \gamma J_- + \sqrt{\frac{\gamma kTJ_+}{\Omega}}\Gamma(t). \tag{IV.5}$$

Stochastic equations (IV.1), (IV.4) and (IV.5) constitute the basic result of the paper, which we use to further analyze dynamical transitions in ABA molecules. To check their accuracy we compare the results of numerical simulations of the original stochastic equations (II.4) with those of Eqs. (IV.1), (IV.4) and (IV.5). The numerical results for the average life time of the antisymmetric normal mode averaged over 1000 trajectories are shown in Fig. 2. Very good agreement is observed between these results. Thus, we use original stochastic equations (II.4) for numerical simulations presented in this paper and compare them with analytical results derived from Eqs. (IV.1), (IV.4) and (IV.5).

From Eq. (IV.1) one can find the equilibrium probability distribution $W_+(J_+)$ for the stochastic variable $J_+$. Eq. (IV.1) corresponds to the Fokker–Planck equation in the form:

$$\frac{\partial \rho_+}{\partial t} = \gamma\left[\frac{\partial}{\partial J_+}\left(J_+ - \frac{2kT}{\Omega}\right) + \frac{\partial^2}{\partial J_+^2}\frac{kTJ_+}{\Omega}\right]\rho_+, \tag{IV.6}$$

which has the following stationary solution:

$$\rho_{+st}(J_+) = \frac{J_+\Omega^2}{(kT)^2}\exp\left(-\frac{J_+\Omega}{kT}\right). \tag{IV.7}$$

Eq. (IV.7) coincides with the energy distribution function of two-dimensional harmonic oscillator, which results from the approximations made so far: the effective decoupling of the equation for $J_+$ and linearization of anharmonic frequencies (in Appendix for the simplification of expressions of non-resonant terms). Since we consider an ABA molecule in thermal equilibrium with bath, $J_+$ is assumed to have reached the stationary distribution (IV.7). One can see that $J_+$ is a random non-Gaussian variable with the average value $\langle J_+\rangle = 2kT/\Omega$ and it plays the role of additional non-Gaussian noise in Eqs. (IV.4) and (IV.5). The distribution function for $J_+$ from the numerical simulations of stochastic equations (II.4) is given in Fig. 3 and agrees with Eq. (IV.7).

### 4.2. Reduced coordinates

We now focus on Eqs. (IV.4) and (IV.5). These equations describe dissipative motion of a rotor in the momentum-dependent cosine potential with Hamiltonian

$$H_{rot} = \frac{J_-^2}{2M} + W_0\sqrt{J_+^2 - J_-^2}\cos(2\psi_-), \tag{IV.8}$$

where $M = \frac{4D}{\Omega^2}$, $W_0 = \frac{|G_{12}|}{G_{11}}\frac{\Omega}{2}$; and parameter $J_+$ is a stochastic variable. In this and following sections, we will extensively use the term "oscillations of rotor" in a cosine potential, which should not be confused with the vibrations of ABA molecules: the former stands for the oscillatory motion in energy space, i.e. one oscillation of rotor corresponds to one complete energy exchange between AB and BA bonds in ABA molecule, while the latter corresponds to the oscillatory motion in coordinate space, i.e. during a single period of rotor's oscillation ABA molecule can perform hundreds of high-frequency vibrations.

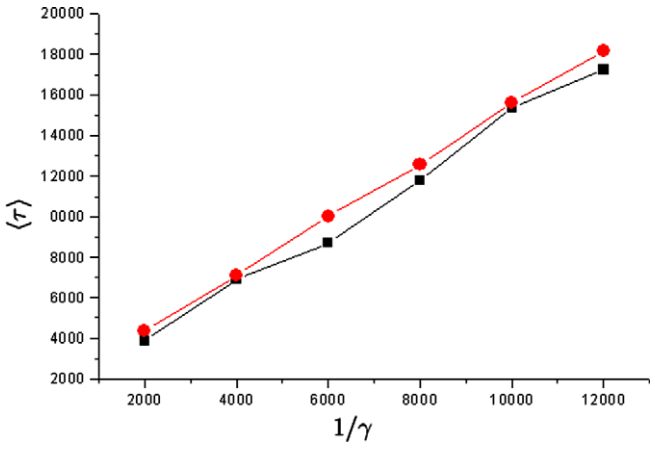


**Fig. 2.** Mean life time of the antisymmetric normal mode of $H_2O$ molecule at $kT/D = 1/100$ as a function of inverse friction in units of $\Omega$. Squares stand for the numerical results obtained from the integration of Eq. (II.4), circles represent the numerical results obtained from the integration of Eqs. (IV.4) and (IV.5).

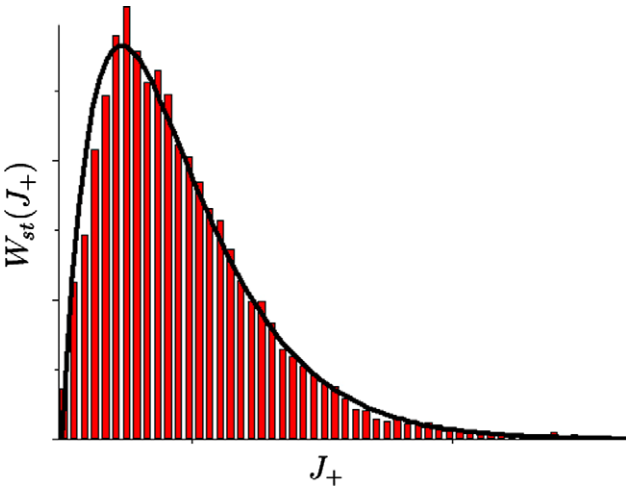


**Fig. 3.** Probability distribution of $J_+$. The histogram represents the result of numerical simulations of Eq. (II.4), and the solid line is the analytical result (IV.7). The values of parameters are chosen to model $H_2O$: $kT/D = 1/75$, $\gamma/\Omega = 1/4000$.

As discussed in paper **I**, the range of rotor energies that correspond to the antisymmetric normal-mode behavior of an ABA molecule is $-W_0 J_+ \leqslant E_{rot} < J_+^2/2M$ and the range of energy for the symmetric normal-mode behavior is $J_+^2/2M < E_{rot} \leqslant W_0 J_+$. When in the presence of dissipation, thermal noise forces the rotor energy $E_{rot}$ to diffuse. When the rotor energy reaches the value $E_{rot}^c = J_+^2/2M$ the cosine potential flips and the antisymmetric-to-symmetric normal mode transition occurs. Noise driven dynamics is governed by stochastic equations (IV.4) and (IV.5). These equations can be further simplified by introducing reduced parameters $j_- \equiv J_-/J_+$ and $h_{rot} \equiv H_{rot}/W_0 J_+$, which instead of original variables $J_-$ and $E_{rot}$, defined on $-J_+ \leqslant J_- \leqslant J_+$ and $-W_0 J_+ \leqslant E_{rot} \leqslant W_0 J_+$, respectively, are now defined on intervals with non-fluctuating boundaries $-1 \leqslant j_- \leqslant 1$ and $-1 \leqslant \varepsilon_{rot} \leqslant 1$. The symmetric-to-antisymmetric normal mode transition occurs at $E_{rot} = J_+^2/2M$ or equivalently at $\varepsilon_{rot} = J_+/2MW_0 = J_+/\widetilde{J}_+^c$. Using the transformations of stochastic variables [14,15], Eqs. (IV.4) and (IV.5) now read (in the Ito form of stochastic calculus)

$$\begin{aligned} \frac{d\psi_-}{dt} &= -W_0 \frac{\partial h_{rot}}{\partial j_-}, \\ \frac{dj_-}{dt} &= W_0 \frac{\partial h_{rot}}{\partial \psi_-} + \sqrt{1+j_-^2}\sqrt{\frac{\gamma kT}{\Omega J_+}}\Gamma(t). \end{aligned} \tag{IV.9}$$

Once $J_+$ has reached equilibrium (see discussions in the previous section) we can set its value in the noise term in Eq. (IV.9) to its equilibrium value $2kT/\Omega$. Also, since $j_-$ oscillates around zero and its magnitude is always $|j_-| \leqslant 1$ (reaching $\pm 1$ only at the point of symmetric-to-antisymmetric normal mode transition) and thus $1+j_-^2 < 1+\frac{1}{2}$, we can set $1+j_-^2$ in the noise term to be approximately equal to 1. Stochastic equation (IV.9) then take a very simple form

$$\begin{aligned} \frac{d\psi_-}{dt} &= -W_0 \frac{\partial h_{rot}}{\partial j_-}, \\ \frac{dj_-}{dt} &= W_0 \frac{\partial h_{rot}}{\partial \psi_-} + \sqrt{\frac{\gamma}{2}}\Gamma(t), \end{aligned} \tag{IV.10}$$

where

$$\langle \Gamma(t)\Gamma(t')\rangle = 2\delta(t-t'), \tag{IV.11}$$

$$h_{rot} = \kappa j_-^2 + \sqrt{1-j_-^2}\cos(2\psi_-), \tag{IV.12}$$

$$\kappa \equiv \frac{kT}{MW_0\Omega} \tag{IV.13}$$

with antisymmetric normal mode corresponding to $-1 < \varepsilon_{rot} < \kappa$ and symmetric normal mode corresponding to $\kappa < \varepsilon_{rot} < 1$. The transition point $\varepsilon_{rot} = \kappa$, an important parameter of the theory, can be compared with direct numerical simulations of original equations (II.4) to check the validity of the approximations made so far. The distribution of energies recorded within a period of rotor's oscillation after the event of symmetric-to-antisymmetric normal mode transition should be obviously peaked at $\varepsilon = \kappa$. Numerical simulations of stochastic equations (II.4) showed that the transition point (the peak) agrees well with expression (IV.13), yet to make it precise the expression, (IV.13) should be slightly modified with coefficient 0.7 (see Fig. 4), giving

$$\kappa = \frac{0.7kT}{MW_0\Omega}. \tag{IV.14}$$

Below in the text we use this expression for $\kappa$ to compare the results of analytical theory with numerical calculations.

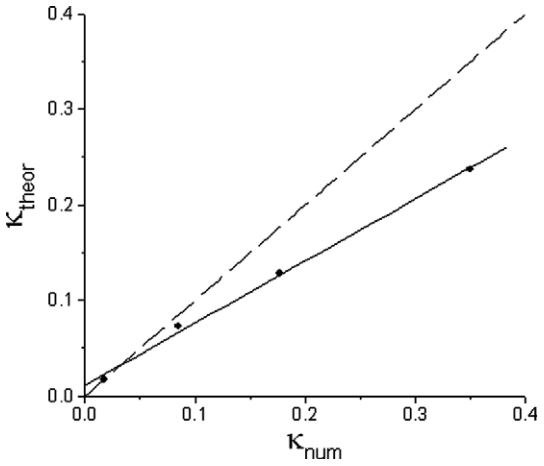


**Fig. 4.** Theoretical values $\kappa_{theor}$ of transition point $\kappa$ versus its numerical values $\kappa_{num}$, obtained from direct integration of stochastic equations (II.4). Dashed line represents bisectrix for comparison.

### 4.3. The diffusion equation for reduced rotor energy $\varepsilon$

In Section 3, we have imposed restrictions to the allowed values of bath temperature $T$ and friction strength $\gamma$, which are set weak enough not to disturb the oscillatory nature of ABA molecule. In the limit of low temperature and friction, the rotor energy $E_{rot}$ changes very slowly during a period of oscillation, so that during a single period of oscillation the motion of rotor can be described by non-dissipative equations $\frac{d\psi_-}{dt} \approx -\frac{\partial H_{rot}}{\partial J_-}$ and $\frac{dJ_-}{dt} \approx \frac{\partial H_{rot}}{\partial \psi_-}$ and are integrated in Appendix B. We therefore can apply the Kramers energy diffusion approach [12]. Following Kramers derivation we write down the Fokker–Planck equation corresponding to stochastic equations (IV.10) and average it over a period of rotor's oscillation, giving

$$\frac{\partial \bar{\rho}}{\partial t} = \overline{\left[-\frac{\partial}{\partial \psi_-}\left(-W_0\frac{\partial h_{rot}}{\partial j_-}\right) - \frac{\partial}{\partial j_-}\left(W_0\frac{\partial h_{rot}}{\partial \psi_-}\right) + \frac{\gamma}{2}\frac{\partial^2}{\partial j_-^2}\right]}\bar{\rho}. \tag{IV.15}$$

In the energy diffusion regime, the distribution density depends only on energy and time, thus $\bar{\rho} = \rho(\varepsilon, t)$. The first two terms on the right side disappear since they correspond to constant-energy motion and the remaining third term results in

$$\frac{\partial \rho(\varepsilon,t)}{\partial t} = \frac{\gamma}{2}\left[\overline{\left(\frac{\partial^2 \varepsilon}{\partial j_-^2}\right)}\frac{\partial \rho(\varepsilon,t)}{\partial \varepsilon} + \overline{\left(\frac{\partial \varepsilon}{\partial j_-}\right)^2}\frac{\partial^2 \rho(\varepsilon,t)}{\partial \varepsilon^2}\right]. \tag{IV.16}$$

The averages of derivatives are performed in Appendix B which transform (IV.16) into

$$\frac{\partial \rho(\varepsilon,t)}{\partial t} = \left[-\frac{\partial}{\partial \varepsilon}D^{(1)}(\varepsilon) + \frac{\partial^2}{\partial \varepsilon^2}D^{(2)}(\varepsilon)\right]\rho(\varepsilon,t), \tag{IV.17}$$

where drift $D^{(1)}$ and diffusion $D^{(2)}$ coefficients are

$$D^{(1)}(\varepsilon) = -\frac{\gamma}{4}\left(1 + \frac{1}{(\varepsilon-\kappa)^2}\right)\mathrm{sign}(\varepsilon-\kappa), \tag{IV.18}$$

$$D^{(2)}(\varepsilon) = \frac{\gamma}{2}\left\{\frac{1}{2}\left(\frac{1-(\varepsilon-\kappa)^2}{|\varepsilon-\kappa|}\right) - \kappa\,\mathrm{sign}(\varepsilon-\kappa)\right\}. \tag{IV.19}$$

This diffusion equation completely describes the statistics of symmetric-to-antisymmetric normal mode stochastic transitions, and thus is the central result of the present paper.

## 5. The lifetime of symmetric and antisymmetric normal modes

### 5.1. Antisymmetric normal mode

The lifetime of the antisymmetric normal mode is the average time $t_A$ that rotor spends in the cosine potential well with the energy $E_{rot} < J_+^2/2M$ or equivalently with energies $\varepsilon_{rot} = \varepsilon$ in the range $-1 \leqslant \varepsilon \leqslant \kappa$. The mean life time of the antisymmetric mode is then the mean first exit time of diffusion process (IV.17) from the region $-1 \leqslant \varepsilon \leqslant \kappa$ with the absorbing boundary condition at $\varepsilon = \kappa$ and reflecting boundary condition at $\varepsilon = -1$. The drift and diffusion coefficients in the case of antisymmetric mode are

$$D^{(1)}(\varepsilon) = \frac{\gamma}{4}\left(1 + \frac{1}{(\varepsilon-\kappa)^2}\right), \tag{V.1}$$

$$D^{(2)}(\varepsilon) = \frac{\gamma}{2}\left\{\frac{1}{2}\left(\frac{(\varepsilon-\kappa)^2-1}{\varepsilon-\kappa}\right) + \kappa\right\}. \tag{V.2}$$

At this point we note that the drift coefficient $D^{(1)}(\varepsilon)$ is always positive, and therefore

$$\left\langle \frac{d\varepsilon}{dt} \right\rangle = D^{(1)}(\varepsilon) > 0, \tag{V.3}$$

i.e. noise drives up the energy of the rotor (which is just the Kramers mechanism of noise-driven escape), or in other words, the ABA molecule tends to escape from antisymmetric normal-mode dynamics.

From (V.1) and (V.2) we immediately find the mean escape time from the interval $-1 \leqslant \varepsilon \leqslant \kappa$ with reflecting boundary at $\varepsilon = -1$ and absorbing boundary at $\varepsilon = \kappa$. If the rotor has initial energy $\varepsilon = \varepsilon_0$ $(-1 \leqslant \varepsilon_0 \leqslant \kappa)$, then the mean first passage time is given by [15]

$$\begin{aligned} t_A(\varepsilon_0) &= 2\int_{\varepsilon_0}^{\kappa} \frac{dy}{\Psi(y)} \int_{-1}^{y} \frac{\Psi(z)}{2D^{(2)}(z)}\, dz = \frac{4}{\gamma}\int_{\varepsilon_0}^{\kappa} \frac{(1+y)(\kappa-y)}{1+\kappa^2-y^2}\, dy \\ &= \frac{1}{\gamma}\left\{ 4(\kappa-\varepsilon_0) + 2(\kappa-1)\ln\left[1+\kappa^2-\varepsilon_0^2\right] \right. \\ &\quad \left. + 2\left(\frac{\kappa-1-\kappa^2}{\sqrt{1+\kappa^2}}\right)\ln\left[\frac{\left(\sqrt{1+\kappa^2}+\kappa\right)\left(\sqrt{1+\kappa^2}-\varepsilon_0\right)}{\left(\sqrt{1+\kappa^2}-\kappa\right)\left(\sqrt{1+\kappa^2}+\varepsilon_0\right)}\right]\right\}, \end{aligned} \tag{V.4}$$

where $\Psi(x) = \exp\left[\int^x \frac{D^{(1)}(x')}{D^{(2)}(x')}\, dx'\right] = \kappa + x + (1/(\kappa - x))$. $t_A(\varepsilon_0)$ is the lifetime of antisymmetric normal mode formed at energy $\varepsilon = \varepsilon_0$ in a thermal bath of temperature $T$ and friction strength $\gamma$. The expression is valid for values of $\kappa$ up to 0.5, and improves if the condition (III.5), i.e. $\kappa \ll 1$, is satisfied.

If we prepare the antisymmetric normal mode at $\varepsilon_0 = -1$, which corresponds to the bottom of rotor's cosine potential, i.e. the case of perfect antiphased oscillations of AB and BA bonds in ABA molecule, $\psi_- = \pi/2$, then this antisymmetric mode according to Eq. (V.4) will last for the duration $t_A(-1) \approx (1.24 + 2.34\kappa - 0.76\kappa^2)/\gamma$, which is approximately $t_A \approx 1.5/\gamma$ for temperatures $\kappa < 0.2$. The weak dependence of $t_A$ on $\kappa$ is the reason for the temperature invariance and AB–BA coupling strength $(W_0)$ invariance of antisymmetric mode lifetime observed in paper **I**. The numerical simulations [16] of dissipative dynamics of ABA molecule governed by Eq. (II.4) with initial condition $\varepsilon_0 = -1$ (see Table 2) are in good agreement with the analytical result (V.4). Analytical Fokker–Planck equation (IV.17) with diffusion coefficients (V.1) and (V.2) also allows to compare the statistics of lifetimes of antisymmetric normal mode. The comparison of analytical distribution curve $p(t) = -\int_{-1}^{\kappa} d\varepsilon \partial\rho(\varepsilon, t)/\partial t$ with the numerical results is shown in Fig. 5 and finds a very good agreement.

**Table 2**
The slopes $\alpha$ for the expression of the mean lifetime $\langle\tau\rangle = \alpha/\gamma$ of symmetric and antisymmetric normal modes, formed at $\varepsilon = 1$ and $\varepsilon = -1$, respectively.

| $kT/D$ | $\alpha_{num}$ | $\alpha_{theor}$ |
|---|---|---|
| *Antisymmetric* | | |
| $\frac{1}{100}$ | 1.44 | 1.77 |
| $\frac{1}{200}$ | 1.33 | 1.52 |
| $\frac{1}{10{,}000}$ | 1.22 | 1.23 |
| *Symmetric* | | |
| $\frac{1}{100}$ | 0.78 | 0.52 |
| $\frac{1}{200}$ | 1.05 | 0.86 |
| $\frac{1}{10{,}000}$ | 1.26 | 1.22 |

The numerical results $\alpha_{num}$ were obtained by plotting mean lifetimes of normal modes versus the inverse friction similar to Fig.2 and the slope of best fit line was taken as $\alpha_{num}$. The theoretical slopes $\alpha_{theor}$ are given by Eqs. (V.4) and (V.8).

### 5.2. Symmetric normal mode

The lifetime of symmetric normal mode is the mean time $t_S$ that the rotor spends in the cosine potential well with energy $E_{rot} > J_+^2/2M$ or equivalently with energies $\varepsilon_{rot} = \varepsilon$ in the range $\kappa \leqslant \varepsilon \leqslant 1$. The average lifetime of symmetric mode is the mean first exit time of the diffusion process (IV.17) from the region $\kappa \leqslant \varepsilon \leqslant 1$ with absorbing boundary condition at $\varepsilon = \kappa$ and reflecting boundary condition at $\varepsilon = 1$. The drift and diffusion coefficients in case of the symmetric mode are now

$$D^{(1)}(\varepsilon) = -\frac{\gamma}{4}\left(1 + \frac{1}{(\varepsilon-\kappa)^2}\right), \tag{V.5}$$

$$D^{(2)}(\varepsilon) = \frac{\gamma}{2}\left\{\frac{1}{2}\left(\frac{1-(\varepsilon-\kappa)^2}{\varepsilon-\kappa}\right) - \kappa\right\}. \tag{V.6}$$

Again, we see that the drift coefficient is always negative, i.e.,

$$\left\langle \frac{d\varepsilon}{dt} \right\rangle = D^{(1)}(\varepsilon) < 0, \tag{V.7}$$

which suggests that noise drives $\varepsilon$ toward the transition point $\varepsilon = \kappa$ and thus plays the role of driving force for the symmetry-breaking (i.e. symmetric-to-antisymmetric normal mode) transition. If the rotor has initial energy $\varepsilon = \varepsilon_0$ $(\kappa \leqslant \varepsilon_0 \leqslant 1)$, then the lifetime of symmetric normal mode is

$$\begin{aligned} t_S(\varepsilon_0) &= 2\int_{\kappa}^{\varepsilon_0} \frac{dy}{\Psi(y)} \int_{y}^{1} \frac{\Psi(z)}{2D^{(2)}(z)}\, dz \\ &= \frac{1}{\gamma}\left\{ 4(\varepsilon_0-\kappa) - 2(\kappa+1)\ln\left[1+\kappa^2-\varepsilon_0^2\right] \right. \\ &\quad \left. + 2\left(\frac{1+\kappa+\kappa^2}{\sqrt{1+\kappa^2}}\right)\ln\left[\frac{\left(\sqrt{1+\kappa^2}+\kappa\right)\left(\sqrt{1+\kappa^2}-\varepsilon_0\right)}{\left(\sqrt{1+\kappa^2}-\kappa\right)\left(\sqrt{1+\kappa^2}+\varepsilon_0\right)}\right]\right\}. \end{aligned} \tag{V.8}$$

where $\Psi(x)$ is the same as in the case of antisymmetric mode. The expression for $t_S(\varepsilon_0)$ improves as the condition (III.5), i.e. $\kappa \ll 1$, is satisfied.

If the symmetric normal mode is formed at $\varepsilon_0 = 1$, which corresponds to the top of rotor's cosine potential and to the case of perfect in-phase oscillations of AB and BA bonds in ABA molecule, $\psi_- = 0$, then such a symmetric mode according to Eq. (V.8) lasts for the duration $t_S(1) \approx (1.24 - 3.54\kappa - 2.6\kappa^2)/\gamma$.

### 5.3. Populations of symmetric and antisymmetric normal modes

From the above analysis, one can also make an important observation that with the increase of temperature (i.e. $\kappa$) the range of

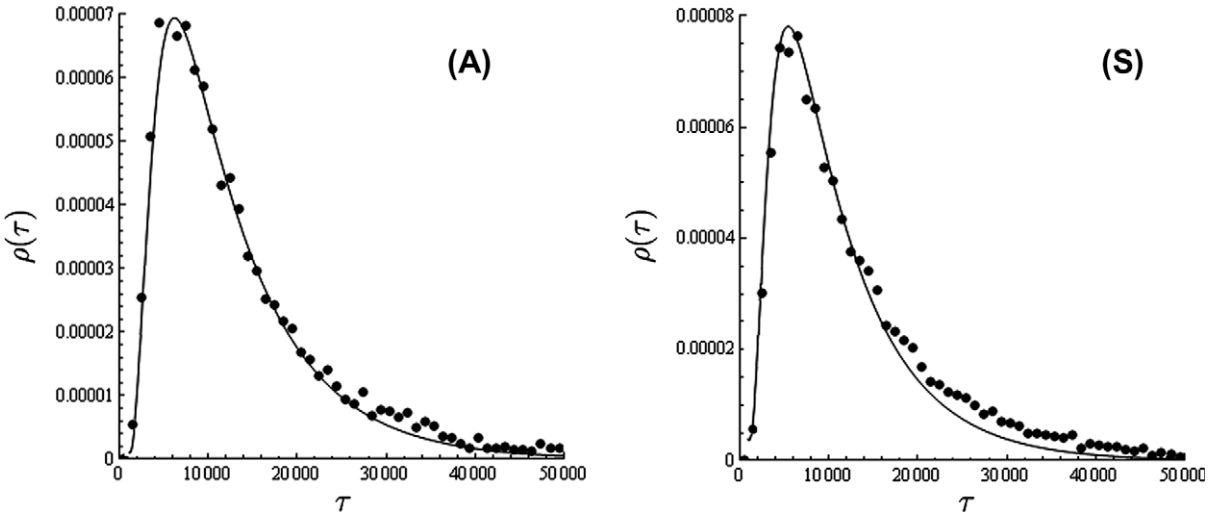


**Fig. 5.** Lifetime distribution function for antisymmetric (A) and symmetric normal mode (S) at $kT/D = 1/1000$ and $\gamma/\Omega = 1/10{,}000$. The antisymmetric normal mode was formed at $\varepsilon = -1$, i.e. perfect antiphase oscillations of HO and OH bonds, while the symmetric normal mode was formed at $\varepsilon = 1$, i.e. perfect inphase oscillations of OH and HO bonds. The unit of time is $1/\Omega$. Dots represent numerical results obtained by integration of stochastic equations (II.4) for the model of $H_2O$ molecule, while solid lines are the analytical distribution functions.

allowed energies for antisymmetric normal mode ($-1 < \varepsilon < \kappa$) increases, while the range of allowed energies for symmetric normal mode ($\kappa < \varepsilon < 1$) decreases and vanishes as $\kappa$ reaches 1. Therefore, one should expect that higher temperatures *destabilize* symmetric normal mode and thus *depopulate* it. This can be shown explicitly by solving the diffusion equation (IV.17). Its stationary (thermal equilibrium) solution is $\rho(\varepsilon) = \frac{1}{2},\ -1 < \varepsilon < 1$. Since antisymmetric (A) normal mode corresponds to $-1 < \varepsilon < \kappa$, and symmetric (S) normal mode corresponds to $\kappa < \varepsilon < 1$, the ratio of their populations $n_A$ and $n_S$ is

$$\frac{n_S}{n_A} = \frac{1-\kappa}{1+\kappa}. \tag{V.9}$$

This simple relation agrees well with the direct numerical simulations of stochastic equations (II.4), see Fig. 6, which was obtained as the ratio between the total amount of time that the model ABA molecule spends in (S) and (A) modes, respectively. One can see,

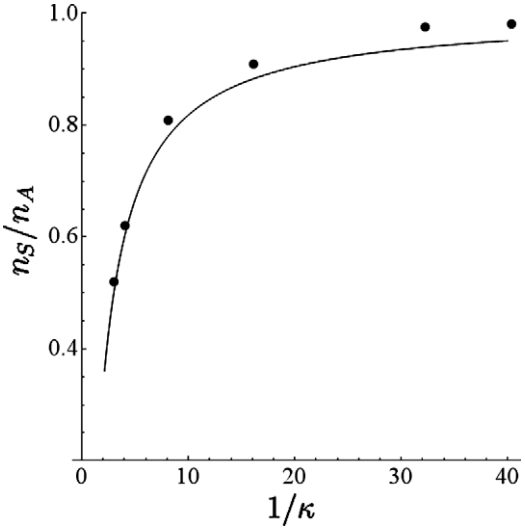


**Fig. 6.** Ratio of equilibrium populations of symmetric and antisymmetric normal modes $n_S/n_A$ of $H_2O$ molecule obtained by integration of Eq. (II.4) (dots) and analytical equation (V.9) (solid line) as a function of inverse temperature.

that higher temperatures, i.e. $\kappa$, *reduce* the ratio (V.9), which is just the opposite to the effect expected in noise-free quantum system (ABA molecule) in which higher temperatures should equilibrate populations of antisymmetric and symmetric normal modes.

## 6. Statistics of symmetry breaking from a single trajectory calculation

In Section 6, we have discussed symmetric-to-antisymmetric normal mode transitions for trajectories with a given initial condition. The statistics of first exit times were collected on a set of trajectories, all with the same initial conditions. Yet, it is more interesting to collect the statistics of the symmetric or antisymmetric state by counting the events along a single trajectory, as in the single molecule experiment. In paper **I**, a single trajectory of $\psi_-(t)$ was observed and analyzed. The statistics of time intervals in either symmetric normal mode or antisymmetric normal mode was then collected and the distribution was found to be of non-Poissonian form. In this section, we provide analytical derivation of the observed statistics.

The statistics of symmetry breaking is governed by diffusion equation (IV.17). Yet, this diffusion equation now needs to be solved with different initial conditions. In this case rotor jumps in and out of its antisymmetric mode region and symmetric mode region entering "from the top", i.e. from the symmetry breaking transition point $\varepsilon = \kappa$ (whereas in the previous section we formed normal mode "near the bottom" of the cosine potential and recorded the times when it jumped out at the transition point $\varepsilon = \kappa$). From the numerical experiment, we can observe only those events that have timescales longer than the period of rotor's oscillation $\tau = \pi/W_0\sqrt{1-2\kappa\varepsilon}$ (see Appendix B). The distribution of $\rho_0(\varepsilon,\tau)$ over the time $\tau$ in the vicinity of transition point $\varepsilon = \kappa$ will be the initial distribution density for the diffusion equation (IV.17) for the comparison with the numerical experiment. We cannot obtain this initial distribution density from the diffusion equation (IV.17) since this equation was obtained by averaging over the period of rotor's oscillation $\tau$, i.e. it does not have enough resolution for times less than a single period of oscillation. Yet, we know that by definition, reduced energy $\varepsilon$ is the ratio of two fluctuating random variables $\varepsilon = E_{rot}/W_0 J_+$. For the time $\tau$, we can assume $E_{rot}$ and $J_+$ to be Gaussian random variables. Then the ratio of the two

normal variables follows the Lorentz distribution and we can therefore immediately get the general form of $\rho_0(\varepsilon,\tau)$

$$\rho_0(\varepsilon,\tau)=\frac{1}{\pi}\frac{\Delta\varepsilon}{(\varepsilon-\kappa)^2+\Delta\varepsilon^2}, \tag{VI.1}$$

which is centered around the transition point $\kappa$ and has the width $\Delta\varepsilon$. This width is obviously determined by the diffusion of $\varepsilon$ during the time $\tau$ and therefore $\Delta\varepsilon^2\sim\gamma\tau$, thus giving the final form of the initial distribution $\rho_0(\varepsilon,\tau)$

$$\rho_0(\varepsilon,\tau)=\frac{1}{\pi}\frac{\sqrt{C\gamma\tau}}{(\varepsilon-\kappa)^2+C\gamma\tau}. \tag{VI.2}$$

We identify the constant coefficient $C$ as the best fit of the theoretical mean life time of antisymmetric normal mode

$$\langle t_A\rangle=\frac{\int_{-1}^{\kappa}t_A(\varepsilon)\rho_0(\varepsilon,\tau)\,d\varepsilon}{\int_{-1}^{\kappa}\rho_0(\varepsilon,\tau)\,d\varepsilon}, \tag{VI.3}$$

where $t_A$ is given by (V.4) and $\rho_0(\varepsilon,\tau)$ is given by (VI.2), to the experimentally observed from numerical simulations of a single trajectory [17] (see Fig. 7). The best fit result gives $C=3.1$. The lifetime $\langle t_A\rangle$ in (VI.3) is the average time that the ABA molecule spends in the antisymmetric normal mode regime obtained by averaging over the events along a single trajectory (see paper **I**). Similarly, the mean time that molecule ABA spends in symmetric normal-mode dynamics is

$$\langle t_S\rangle=\frac{\int_{\kappa}^{1}t_S(\varepsilon)\rho_0(\varepsilon,\tau)\,d\varepsilon}{\int_{\kappa}^{1}\rho_0(\varepsilon,\tau)\,d\varepsilon}, \tag{VI.4}$$

where $t_S(\varepsilon)$ is given by (V.8). The analytical results (VI.3) and (VI.4) with the fixed value $C=3.1$ agree well with the whole set of numerical results obtained for different temperatures $T$ and coupling strengths $W_0$.

We can now derive the analytical distribution functions of the lifetimes $t_A$ and $t_S$. First, we solve the diffusion equation (IV.17) on the interval $-1\leqslant\varepsilon\leqslant\kappa$ with the boundary conditions $\partial\rho(-1,t)/\partial\varepsilon=0$, $\rho(\kappa,t)=0$ and initial condition $\rho(\varepsilon,0)=\rho_0(\varepsilon,\tau)\big/\int_{-1}^{\kappa}\rho_0(\varepsilon,\tau)\,d\varepsilon$. To set the initial condition in accord with the boundary conditions we introduce small correction to the curvature of $\rho(\varepsilon,0)$ at $\varepsilon=-1$ and set $\rho(\varepsilon,0)=0$ for $|\varepsilon-\kappa|<0.01$. The distribution function of first exit times through the boundary $\varepsilon=\kappa$, i.e. $\rho(t_A)$, is then

$$\rho(t)=-\int_{-1}^{\kappa}\frac{\partial\rho(\varepsilon,t)}{\partial t}\,d\varepsilon. \tag{VI.5}$$

In principle, the diffusion equation (IV.17) with coefficients (V.1) and (V.2) can be solved by separation of variables, the solution can be then substituted in (VI.5) to get the analytical expression. Yet, the analytical expression is not much simpler than the direct numerical integration of (IV.17) and (VI.5). The obtained result is shown in Fig. 8 and results in a good agreement with the statistics of lifetimes obtained by direct integration of the original stochastic equations (II.4) (see paper **I**).

The analytical distribution function for the lifetimes of symmetric normal mode is obtained in a similar way by solving the diffusion equation (IV.17) on the interval $\kappa\leqslant\varepsilon\leqslant1$ with the boundary conditions $\partial\rho(1,t)/\partial\varepsilon=0$, $\rho(\kappa,t)=0$ and initial condition $\rho(\varepsilon,0)=\rho_0(\varepsilon,\tau)\big/\int_{\kappa}^{1}\rho_0(\varepsilon,\tau)\,d\varepsilon$. The results are presented in Fig. 8.

## 7. Discussions

In the present paper, we have analyzed the statistics of symmetry-breaking dynamical transitions in ABA molecules, i.e. the noise-induced transitions between the symmetric and antisymmetric normal modes. Normal mode oscillation of ABA molecules formed at thermal equilibrium with bath is forced to switch its symmetry under the influence of noise. The dynamical "blinking" phenomena therefore originates.

The mean lifetimes of both normal modes were obtained analytically as a function of AB–BA bond coupling strength and the parameters of environment such as temperature and friction. At the temperatures much lower than the critical decoupling temperature (the temperature which decouples AB and BA bonds, see text) the lifetimes of both normal modes do not depend either on temperature $T$ of the thermal environment or AB–BA coupling strength $W_0$ and are equal to $1.24/\gamma$, where $\gamma$ is a friction strength. At higher temperatures, yet still lower than the decoupling temperature, the lifetime of symmetric normal modes decreases and may eventually become zero, while the lifetime of antisymmetric normal mode increases very slowly. The later observation illustrates the result discussed in paper **I** that symmetric normal mode is stable only at moderate temperatures, while antisymmetric normal mode is stable at any temperature. We have also studied analytically the statistics of symmetry breaking transitions and

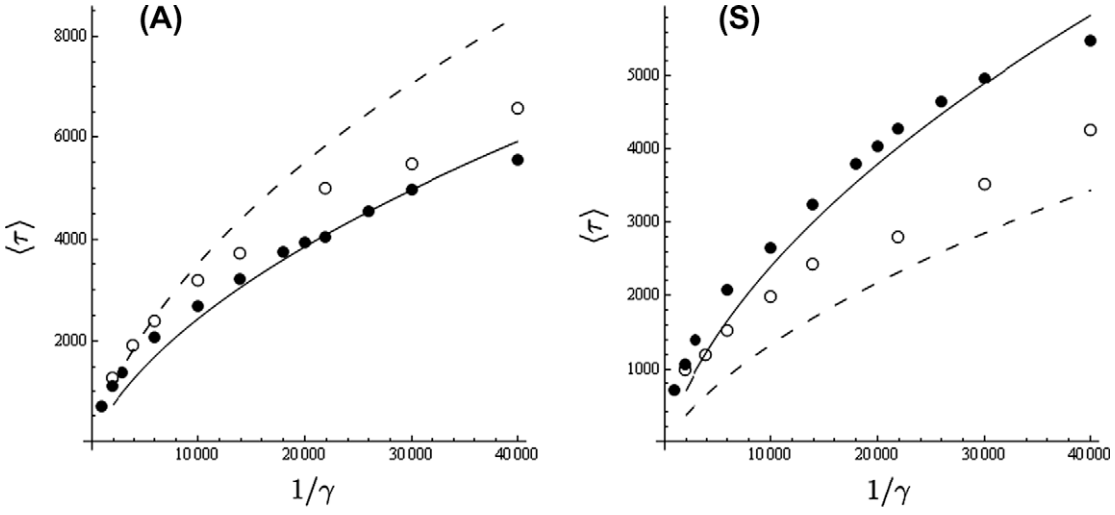


**Fig. 7.** The mean lifetimes of antisymmetric (A) and symmetric (S) normal modes observed from a single trajectory as a function of inverse friction $1/\gamma$. The unit of time is $1/\Omega$. Solid circles represent numerical results for the $H_2O$ model and $kT/D=1/5000$, open circles represent numerical results for $kT/D=1/200$. Lines represent analytical results with best-fit coefficient $C=3.1$: solid line stands for $kT/D=1/5000$, dashed line stands for $kT/D=1/200$.

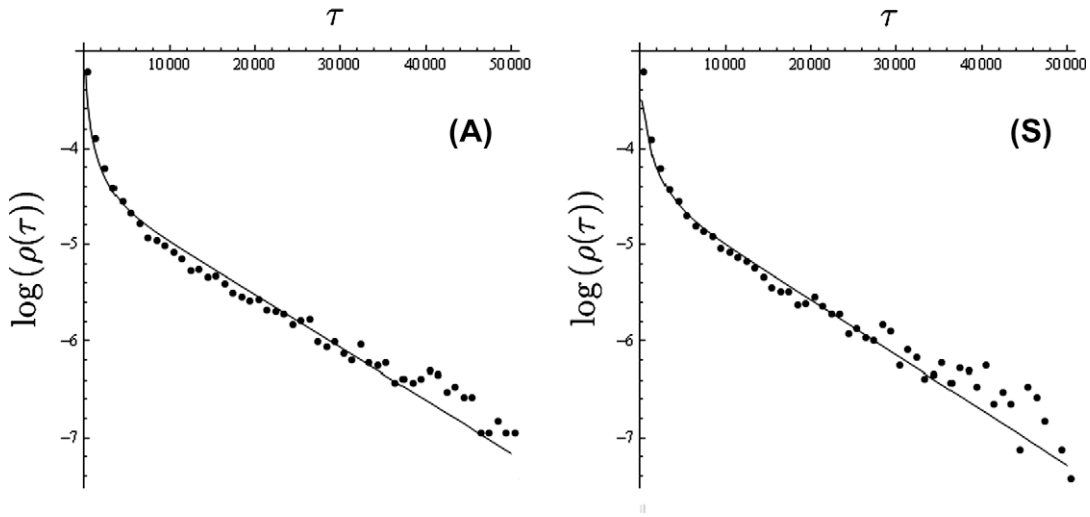


**Fig. 8.** Lifetime distribution functions for antisymmetric (A) and symmetric normal modes (S) at $kT/D = 1/1000$ and $\gamma/\Omega = 1/10{,}000$ along a single trajectory. The units of time is $1/\Omega$. Dots represent numerical results obtained by integration of stochastic equations (II.4) for the model of $H_2O$ molecule, while solid lines are the analytical distribution functions.

obtained non-Poissonian lifetime distribution observed in paper **I**. The reason for non-Poissonian statistics is the underlying energy diffusion mechanism, which results in multiple exponential decays of the first passage time statistics.

The theory developed in the present paper, although being classical, may have an important implications in modern chemistry that deals with single molecule experiments suggesting a possible mechanism of blinking phenomena from the first principles.


## Acknowledgement

This work is supported by ARO under grant W911NF-09-1-0480, NSF CHE 0806266, and MITEI seed grant. We dedicate this paper to Professor Eli Pollak with admiration. His work on chemical dynamics has influenced many of our papers.


## Appendix A

In this appendix, we perform the averaging of Eq. (II.7) over $\psi_+$. Everywhere below the bar means averaging over $\psi_+$:

(I)

$$\begin{aligned}\overline{\widehat{L}\rho} = \overline{\{\rho, H_s\}} &= \overline{\frac{\partial\rho}{\partial\psi_-}\frac{\partial H_s}{\partial J_-}} - \overline{\frac{\partial\rho}{\partial J_-}\frac{\partial H_s}{\partial\psi_-}} + \overline{\frac{\partial\rho}{\partial\psi_+}\frac{\partial H_s}{\partial J_+}} \\ &= \frac{\partial\bar\rho}{\partial\psi_-}\frac{\partial H_s}{\partial J_-} - \frac{\partial\bar\rho}{\partial J_-}\frac{\partial H_s}{\partial\psi_-} \equiv \{\bar\rho, H_s\}_-,\end{aligned} \tag{A.1}$$

where the ABA-molecule's Hamiltonian in action-angle variables $H_s$ is given by Eq. (II.9).

(II) To average irreversible terms in (II.7) over $\psi_+$ we recall that the parameters of thermal bath that we are considering are weak $kT \ll D$ and $\gamma \ll \Omega$ and thus each period of oscillation occurs almost at constant energy (or constant action variable), therefore we can follow Kramers derivation to express averaged irreversible terms in action variables:

$$\begin{aligned}\overline{(\widehat{L}_{irr1} + \widehat{L}_{irr2})\rho} &= \gamma\overline{\frac{\partial}{\partial p_1}\left(p_1\rho + \frac{kT}{G_{11}}\frac{\partial\rho}{\partial p_1}\right)} + \gamma\overline{\frac{\partial}{\partial p_2}\left(p_2\rho + \frac{kT}{G_{11}}\frac{\partial\rho}{\partial p_2}\right)} \\ &= \gamma\overline{\frac{\partial}{\partial p_1}\left(p_1\bar\rho + \frac{kT}{G_{11}}\frac{\partial E_1}{\partial p_1}\frac{\partial\bar\rho}{\partial E_1}\right)} + \gamma\overline{\frac{\partial}{\partial p_2}\left(p_2\bar\rho + \frac{kT}{G_{11}}\frac{\partial E_2}{\partial p_2}\frac{\partial\bar\rho}{\partial E_2}\right)} \\ &= \gamma\frac{\partial}{\partial J_1}\left(J_1\bar\rho + \frac{kTJ_1}{\omega_1}\frac{\partial\bar\rho}{\partial J_1}\right) + \gamma\frac{\partial}{\partial J_2}\left(J_2\bar\rho + \frac{kTJ_2}{\omega_2}\frac{\partial\bar\rho}{\partial J_2}\right),\end{aligned} \tag{A.2}$$

where in the last step we used the fact that averaging over $\psi_+$ for one-dimensional operators $L_{irr1}$ and $L_{irr2}$ is the same as averaging over $\varphi_1$ and $\varphi_2$, respectively. We also used that $\frac{\partial}{\partial p_i} = G_{11}p_i\frac{\partial}{\partial E_i}$.

(III) Using the relation $\frac{\partial}{\partial p_i} = G_{11}p_i\frac{\partial}{\partial E_i}$ we write down the average of the last term in (II.7):

$$\begin{aligned}\overline{\gamma\frac{G_{12}}{G_{11}}\left(p_1\frac{\partial}{\partial p_2} + p_2\frac{\partial}{\partial p_1}\right)\rho} &= \gamma G_{12}\left(p_1p_2\frac{\partial}{\partial E_2} + p_2p_1\frac{\partial}{\partial E_1}\right)\bar\rho \\ &= \gamma G_{12}p_1p_2\left(\frac{1}{\omega_1}\frac{\partial}{\partial J_1} + \frac{1}{\omega_2}\frac{\partial}{\partial J_2}\right)\bar\rho \\ &= \gamma V_0 \\ &\quad\times\cos(2\psi_-)\left(\frac{1}{\omega_1}\frac{\partial}{\partial J_1} + \frac{1}{\omega_2}\frac{\partial}{\partial J_2}\right)\bar\rho,\end{aligned} \tag{A.3}$$

where, see paper **I**,

$$G_{12}p_1p_2 = V_0\cos(\varphi_1 - \varphi_2) \tag{A.4}$$

and

$$V_0 = \frac{4DG_{12}}{\Omega^2G_{11}}\omega_1\omega_2\left(\frac{1-\frac{\omega_1}{\Omega}}{1+\frac{\omega_1}{\Omega}}\right)^{1/2}\left(\frac{1-\frac{\omega_2}{\Omega}}{1+\frac{\omega_2}{\Omega}}\right)^{1/2}. \tag{A.5}$$

Combining (A.1)–(A.3) we get the following averaged over $\psi_+$ Kramers equation (II.7):

$$\begin{aligned}\frac{\partial\bar\rho}{\partial t} &= -\{H_s, \bar\rho\}_- + \gamma\frac{\partial}{\partial J_1}\left(J_1\bar\rho + \frac{kTJ_1}{\omega_1}\frac{\partial\bar\rho}{\partial J_1}\right) + \gamma\frac{\partial}{\partial J_2}\left(J_2\bar\rho + \frac{kTJ_2}{\omega_2}\frac{\partial\bar\rho}{\partial J_2}\right) \\ &\quad + \gamma V_0\cos(2\psi_-)\left(\frac{1}{\omega_1}\frac{\partial}{\partial J_1} + \frac{1}{\omega_2}\frac{\partial}{\partial J_2}\right)\bar\rho.\end{aligned} \tag{A.6}$$

We are considering the case of thermal equilibrium of our ABA system, which means that energy of each oscillator $E_i \sim kT \ll D$ and therefore the equilibrium motion will occur mostly in the bottom of Morse potential, therefore to a good degree of accuracy we can set frequencies $\omega_i = \Omega\left(1 - \frac{J}{J_b}\right)$ in Eq. (A.6) to be equal to $\Omega$, which would simplify further analysis of (A.6) a lot:

$$\begin{aligned}\frac{\partial\bar\rho}{\partial t} &= -\{H_s, \bar\rho\}_- + \gamma\frac{\partial}{\partial J_1}\left(J_1\bar\rho + \frac{kTJ_1}{\Omega}\frac{\partial\bar\rho}{\partial J_1}\right) + \gamma\frac{\partial}{\partial J_2}\left(J_2\bar\rho + \frac{kTJ_2}{\Omega}\frac{\partial\bar\rho}{\partial J_2}\right) \\ &\quad + \frac{\gamma V_0}{\Omega}\cos(2\psi_-)\left(\frac{\partial}{\partial J_1} + \frac{\partial}{\partial J_2}\right)\bar\rho.\end{aligned} \tag{A.7}$$

Using transformations (II.8) we express (A.7) in $\{\psi_-, J_-, \psi_+, J_+\}$ variables:

$$\frac{\partial\bar{\rho}}{\partial t} = -\{H_s,\bar{\rho}\}_- + \gamma\left[1+\left(1+\frac{G_{12}}{G_{11}}\cos(2\psi_-)\right)J_+\frac{\partial}{\partial J_+} - \frac{2kT}{\Omega}\frac{\partial}{\partial J_+}\right]\bar{\rho} + \gamma\frac{\partial}{\partial J_-}(J_-\bar{\rho}) + \frac{\gamma kT}{\Omega}\left(\frac{\partial^2}{\partial J_+^2}(J_+\bar{\rho}) + 2\frac{\partial^2}{\partial J_+\partial J_-}(J_-\bar{\rho}) + \frac{\partial^2}{\partial J_-^2}(J_+\bar{\rho})\right). \tag{A.8}$$

Since $G_{12}/G_{11} \ll 1$ (for $H_2O$ it is approximately 1/62), then we can set $\left(1+\frac{G_{12}}{G_{11}}\cos(2\psi_-)\right) = 1$ in the above equation and thus obtain:

$$\frac{\partial\bar{\rho}}{\partial t} = -\{H_s,\bar{\rho}\}_- + \gamma\frac{\partial}{\partial J_+}\left(J_+ - \frac{2kT}{\Omega}\right)\bar{\rho} + \gamma\frac{\partial}{\partial J_-}(J_-\bar{\rho}) + \frac{\gamma kT}{\Omega}\left(\frac{\partial^2}{\partial J_+^2}(J_+\bar{\rho}) + 2\frac{\partial^2}{\partial J_+\partial J_-}(J_-\bar{\rho}) + \frac{\partial^2}{\partial J_-^2}(J_+\bar{\rho})\right), \tag{A.9}$$

## Appendix B

In this appendix, we derive equations for constant-energy oscillations of hindered rotor and provide expressions for several derivatives averaged over a period of rotor's oscillation.

The Hamiltonian under consideration (IV.12) is

$$h = \kappa j_-^2 + \sqrt{1-j_-^2}\cos(2\psi_-) \tag{B.1}$$

with non-dissipative equations of motion (IV.10)

$$\frac{d\psi_-}{dt} = -W_0\frac{\partial h}{\partial j_-}, \qquad \frac{dj_-}{dt} = W_0\frac{\partial h}{\partial \psi_-}. \tag{B.2}$$

Equation for $j_-(t)$ can be integrated substituting cosine function from the expression of Hamiltonian at constant energy $h = \varepsilon$. This results in the approximate expression for $j_-(t)$ valid to the order of $o(\kappa^2)$

$$j_-(t) = \sqrt{\frac{1-\varepsilon^2}{1-2\kappa\varepsilon}}\sin\left[\left(2W_0\sqrt{1-2\kappa\varepsilon}\right)t + \delta_0\right], \tag{B.3}$$

where $\delta_0$ is some initial phase. Coordinate $\psi_-(t)$ then changes as

$$\cos(2\psi_-(t)) = \frac{\varepsilon - \kappa j_-(t)^2}{\sqrt{1-j_-(t)^2}}. \tag{B.4}$$

The period of rotor's oscillation is therefore

$$\tau(\varepsilon) = \frac{\pi}{W_0\sqrt{1-2\kappa\varepsilon}}. \tag{B.5}$$

One can see that for negative $\varepsilon$ period $\tau$ decreases with increasing $\kappa$, while for positive $\varepsilon$ period $\tau$ increases with increasing $\kappa$. It is interesting that since $\kappa$ is proportional to temperature (see text) then higher temperature increases the rate of AB–BA bond energy exchange in antisymmetric normal mode oscillation and decreases it in symmetric normal mode oscillation.

Below we list expressions for averaged over the period $\tau(\varepsilon)$ derivatives $(\partial h/\partial j_-)^2$ and $\partial^2 h/\partial j_-^2$ used in text. These averages can be obtained analytically only for $\kappa = 0$, yet do not have explicit analytical form for $\kappa > 0$. It is interesting though, that their approximate analytical form can be obtained by shifting singularity point of expressions obtained for $\kappa = 0$ from $\varepsilon = 0$ to $\varepsilon = \kappa$. For $\kappa = 0$ we can easily get

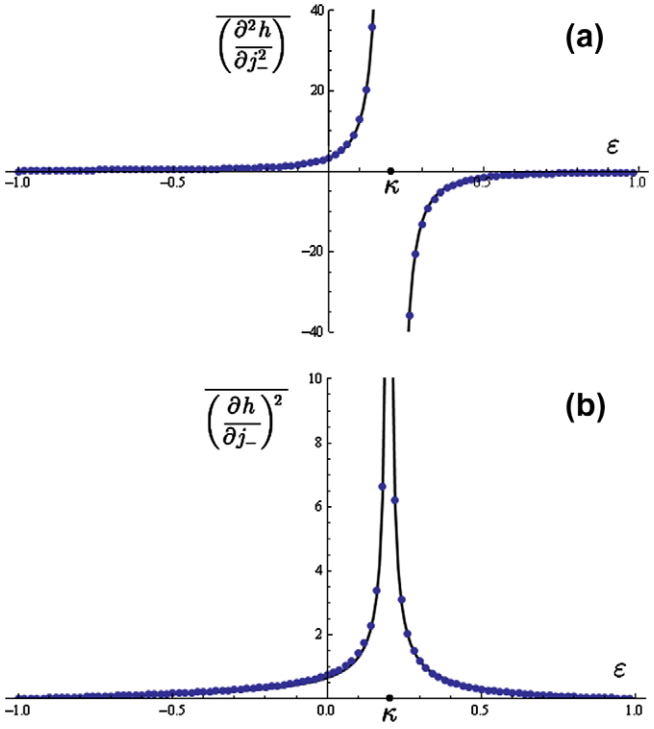


**Fig. 9.** Exact (dots) and approximate (solid lines) averaged derivatives as a function of $\varepsilon$ for $\kappa = 0.2$. (a) average of second derivative; (b) average of squared first derivative.

$$\overline{\left(\frac{\partial^2 h}{\partial j_-^2}\right)}_{\kappa=0} = \frac{1}{\tau}\int_0^\tau\left(\frac{\partial^2 h}{\partial j_-^2}\right)dt = -\frac{W_0}{\pi}\int_0^\tau\frac{\varepsilon\,dt}{\left[1-(1-\varepsilon^2)\sin^2(2W_0t)\right]^2} = -\frac{1}{2}\left(1+\frac{1}{\varepsilon^2}\right)\mathrm{sign}(\varepsilon) \tag{B.6}$$

with $\mathrm{sign}(\varepsilon) = \varepsilon/|\varepsilon|$. For non-zero $\kappa$ we simply replace $\varepsilon$ with $\varepsilon - \kappa$ to get the approximate expression

$$\overline{\left(\frac{\partial^2 h}{\partial j_-^2}\right)} = -\frac{1}{2}\left(1+\frac{1}{(\varepsilon-\kappa)^2}\right)\mathrm{sign}(\varepsilon-\kappa). \tag{B.7}$$

This approximate expression reproduces exact integral very well, see Fig. 9a. In the same way we find expression for the averaged over the period squared first derivative

$$\overline{\left(\frac{\partial h}{\partial j_-}\right)^2}_{\kappa=0} = \frac{1}{\tau}\int_0^\tau\left(\frac{\partial h}{\partial j_-}\right)^2 dt = \frac{1}{\tau}\int_{\psi_-(0)}^{\psi_-(\tau)}\frac{\partial h}{\partial j_-}\,d\psi_- = -\frac{1}{\pi}\int_{\psi_-(0)}^{\psi_-(\tau)}\frac{\varepsilon j_-}{1-j_-^2}\,d\psi_- = \frac{1}{2}\left(\frac{1-\varepsilon^2}{|\varepsilon|}\right). \tag{B.8}$$

And for non-zero $\kappa$'s

$$\overline{\left(\frac{\partial h}{\partial j_-}\right)^2} = \frac{1}{2}\left(\frac{1-(\varepsilon-\kappa)^2}{|\varepsilon-\kappa|}\right) - \kappa\,\mathrm{sign}(\varepsilon-\kappa), \tag{B.9}$$

where the last term appears to keep the expression non-negative on the order of $O(\kappa)$. The approximate result (B.9) is compared to exact in Fig. 9b for $\kappa = 0.2$. It should be also noted here that expression (B.7) can be obtained by differentiation of Eq. (B.9) over $\varepsilon$ (except at the point $\varepsilon = \kappa$, which we can exclude from our analysis).

## References

[1] M. Kryvohuz, J. Cao, J. Phys. Chem., submitted for publication.
[2] C.J. Margulis, D.F. Coker, R.M. Lynden-Bell, J. Chem. Phys. 114 (2001) 67.
[3] G.M. Schmid, S.L. Coy, R.W. Field, R.J. Silbey, J. Chem. Phys. 101 (1994) 869.

[4] P. Hanggi, P. Talkner, M. Borkovec, Rev. Mod. Phys. 62 (1990) 251.
[5] D.K. Campbell, S. Flach, Y.S. Kivshar, Phys. Today 57 (2004) 3, and references inside.
[6] E.L. Sibert, W.P. Reinhardt, J.T. Hynes, J. Chem. Phys. 77 (1982) 3583.
[7] E.L. Sibert, J.T. Hynes, W.P. Reinhardt, J. Chem. Phys. 77 (1982) 3595.
[8] K. Stefanski, E. Pollak, J. Chem. Phys. 87 (1987) 079.
[9] Z. Li, L. Xiao, M.E. Kellman, J. Chem. Phys. 92 (1990) 2251.
[10] D.C. Rouben, G.S. Ezra, J. Chem. Phys. 103 (1995) 1375.
[11] M.E. Kellman, J. Chem. Phys. 83 (1985) 3843.
[12] H.A. Kramers, Physica 7 (1940) 284.
[13] C. Jaffe, P. Brumer, J. Chem. Phys. 73 (1980) 5646.
[14] H. Risken, The Fokker–Planck Equation. Methods of Solution and Applications, Springer-Verlag, Berlin/Heidelberg/New York/Tokyo, 1984.
[15] C.W. Gardiner, Handbook of Stochastic Methods for Physics, Chemistry and the Natural Sciences, Springer-Verlag, Berlin/Heidelberg, 2004.
[16] The numerical integration was performed using Euler integration scheme. The statistics was collected on 1000 trajectories. Every stochastic trajectory originated at the same initial conditions $\psi_-(0) = \pi/2$, $J_- = 0$, and was stopped at the moment of time when it crossed the points $\psi_- = 0$ or $\psi_- = \pi$.
[17] The numerical procedure is described in paper **I**: the type of normal mode is traced by checking which of the equilibrium points $\pi n/2$ are crossed by the process $\psi_-(t)$.